

Hypothetical High-Surface-Area Carbons with Exceptional Hydrogen Storage Capacities: Open Carbon Frameworks

Bogdan Kuchta,^{*,†,‡,§} Lucyna Firlej,^{†,§} Ali Mohammadhosseini,[‡] Pascal Boulet,[‡] Matthew Beckner,[†] Jimmy Romanos,[†] and Peter Pfeifer[†]

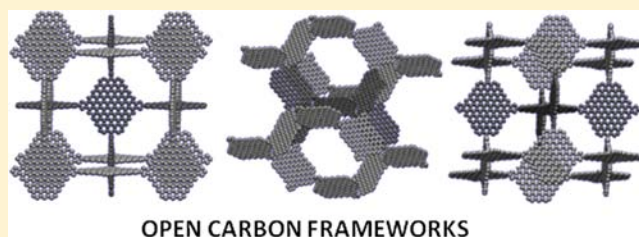
[†]Department of Physics and Astronomy, University of Missouri, Columbia, Missouri 65211, United States

[‡]Laboratoire MADIREL, Université Aix-Marseille, 13396 Marseille, France

[§]Laboratoire Charles Coulombs, Université Montpellier 2, 34095 Montpellier, France

S Supporting Information

ABSTRACT: A class of high-surface-area carbon hypothetical structures has been investigated that goes beyond the traditional model of parallel graphene sheets hosting layers of physisorbed hydrogen in slit-shaped pores of variable width. The investigation focuses on structures with locally planar units (unbounded or bounded fragments of graphene sheets), and variable ratios of in-plane to edge atoms. Adsorption of molecular hydrogen on these structures was studied by performing grand canonical Monte Carlo simulations with



appropriately chosen adsorbent–adsorbate interaction potentials. The interaction models were tested by comparing simulated adsorption isotherms with experimental isotherms on a high-performance activated carbon with well-defined pore structure (approximately bimodal pore-size distribution), and remarkable agreement between computed and experimental isotherms was obtained, both for gravimetric excess adsorption and for gravimetric storage capacity. From this analysis and the simulations performed on the new structures, a rich spectrum of relationships between structural characteristics of carbons and ensuing hydrogen adsorption (structure–function relationships) emerges: (i) Storage capacities higher than in slit-shaped pores can be obtained by fragmentation/truncation of graphene sheets, which creates surface areas exceeding of 2600 m²/g, the maximum surface area for infinite graphene sheets, carried mainly by edge sites; we call the resulting structures open carbon frameworks (OCF). (ii) For OCFs with a ratio of in-plane to edge sites ≈ 1 and surface areas 3800–6500 m²/g, we found record maximum excess adsorption of 75–85 g of H₂/kg of C at 77 K and record storage capacity of 100–260 g of H₂/kg of C at 77 K and 100 bar. (iii) The adsorption in structures having large specific surface area built from small polycyclic aromatic hydrocarbons cannot be further increased because their energy of adsorption is low. (iv) Additional increase of hydrogen uptake could potentially be achieved by chemical substitution and/or intercalation of OCF structures, in order to increase the energy of adsorption. We conclude that OCF structures, if synthesized, will give hydrogen uptake at the level required for mobile applications. The conclusions define the physical limits of hydrogen adsorption in carbon-based porous structures.

■ INTRODUCTION

Hydrogen is an important future energy carrier because it contains the highest energy density (142 MJ/kg) among other fuel sources and burns to produce only water. The most technologically demanding storage is required for mobile (vehicular) applications, where the ultimate tank should provide gravimetric and volumetric densities of at least 7.5 wt % and 70 g/L, respectively. These numbers, defined by the U.S. Department of Energy,¹ are most frequently used as a reference when hydrogen storage is discussed. Several storage options are being studied: compression at high pressure, low-temperature (cryogenic) storage, and different ways of solid storage: physisorption, chemisorption, or chemical compound formation.² Currently, neither option meets all technologically required conditions.

The relatively low heat of hydrogen physisorption in carbon materials (4–6 kJ/mol for adsorption on graphite) and weak

H₂–H₂ interactions limit the total amount of hydrogen stored in porous carbons.³ At room temperature, the adsorption is limited to only one layer. As a consequence, porous (activated) carbons cannot reach the storage level required for practical applications.⁴ This issue has been widely studied and discussed in both experimental and theoretical papers.^{3–15} All studies converge to the same conclusion: to improve hydrogen storage capacity in activated carbons, the adsorbing surfaces must be modified,¹⁶ either by substitution or by doping/intercalation with other species. We discussed some aspects of influence of energetic heterogeneity of sorbent on gas adsorption in our previous papers.^{4,15,17} In particular, the effect of substituting some carbon atoms in the graphene walls by boron atoms^{18,19} on hydrogen storage was studied.²⁰ Our theoretical predictions

Received: July 10, 2012

Published: August 16, 2012

of enhanced adsorption energy in such structures have been confirmed since then by independent experimental data.²¹ Atoms' substitution affects mainly the energy landscape of sorbent;^{20,22,23} however, the induced modifications of adsorption energy appear to be not sufficient to reach required storage capacity, especially for mobile applications. Therefore, it remains important to look at other options^{24–26} and new ideas to prepare the ultimate storage material.

Another way toward higher adsorption capacity would be to increase the specific area of the adsorbent.^{3,12} This strategy has been already applied when preparing metal organic frameworks (MOF),^{27,28} covalent organic frameworks^{29,30} (COF), and porous aromatic frameworks (PAF).³¹ Among carbon-based sorbents, PAFs should potentially show the highest adsorption capacity due to their high specific surface (more than 7000 m²/g), but their energy of adsorption is low; on average, lower than that of activated carbons.

Theoretically, it is possible to conceive an activated carbon with high specific surface area. We focus our discussion on this aspect in the present paper and look for high-surface-area all-carbon adsorbent geometries going beyond the slitlike form: heterogeneous slits; square, triangular, and cylindrical pores; and all possible mixed geometries. We emphasize the physical limits of hydrogen adsorption in these structures and show that this strategy seems to be the only possible solution to prepare an efficient sorbent for hydrogen storage by physisorption.

The data used in this paper as our current experimental reference have been measured on one of the best-performing activated carbon reported in the literature.⁵ However, even the best carbons do not attain the required adsorption uptake and still need additional engineering. The analysis proposed in this paper aims at better understanding its properties and finding a way to modify or define a porous structure with the required properties. This includes a search for optimum pore geometry and pore size/shape distributions. What would an activated carbon with much higher accessible surface than the surface of infinite graphene layer look like? What would the best-performing pore geometry be? The strategy proposed below attempts to answer these questions.

The paper has the following structure. We begin with presentation and analysis of experimental hydrogen adsorption isotherms in our best-performing activated carbons. Then we use simulations of hydrogen adsorption in slit carbon pores to interpret the experimental data. This analysis allows us to validate and calibrate the interaction model that is used in the main part of the paper to test new hypothetical porous carbons. The motivation of this study can be summarized by the following question: is it possible to invent a carbon-based structure that will adsorb enough hydrogen for possible mobile applications? Currently such a structure does not exist. If the answer is yes, then the second question arises: what should be the structural properties of such a material? Trying to answer these two questions, we introduce a notion of open carbon frameworks (OCF) and analyze the properties of several OCF hypothetical structures.

EXPERIMENTAL SECTION

All samples of nanoporous carbons considered in this paper were prepared in granular form by controlled pyrolysis of ground corncob, via a proprietary multistep method.^{5,32} Gravimetric and volumetric hydrogen uptakes (hydrogen 99.999% pure, run through a Matheson Trigas 450B gas purifier for gravimetric measurements) were measured as excess adsorption on a Hiden IGA-001 sorption analyzer and Hiden

HTP1 sorption analyzer, respectively (Hiden Isochema Ltd.). The total amount stored, m_{st} (mass of adsorbed and nonadsorbed hydrogen in the pore space) has been then calculated from the excess adsorption data by use of the formula

$$m_{st} = m_{ads}^e + (\rho_a^{-1} - \rho_s^{-1})\rho_{gas}m_s \quad (1)$$

where ρ_a , ρ_s , ρ_{gas} , and m_s are respectively sample apparent density (including pore space), sample skeletal density (without pore space), density of bulk gas, and sample mass. Figure 1 shows excess adsorption

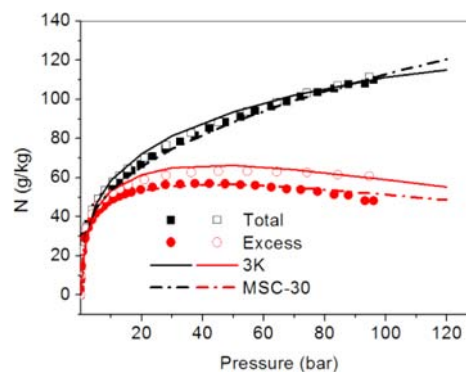


Figure 1. Experimental isotherms of hydrogen adsorption ($T = 80$ K) measured in the Missouri sample (3K, open symbols) and in commercial samples (MCS-30, closed symbols). The lines represent fits calculated from grand canonical Monte Carlo simulations data.

(direct experimental result, in grams of H₂/kilograms of C) and total amount stored (calculated from eq 1, with $\rho_a = 0.5$ g/cm³ and $\rho_s = 2.0$ g/cm³) for two samples: one of the best-performing carbons, prepared at the University of Missouri, and MSC-type carbons.⁹ The relatively high adsorption observed in both cases is a consequence of large specific surface of the samples and it confirms the high quality of activated carbon produced in our laboratory.⁵

NUMERICAL TECHNIQUE

To simulate the interaction of hydrogen molecules with pore walls, 3D adsorbate–adsorbent energy grids were calculated and implemented in our grand canonical Monte Carlo (GCMC) Fortran code. The model of H₂–graphene interaction assumes that H₂ molecule interacts with all carbon atoms through 6–12 Lennard-Jones potential. H₂ molecules were considered as structureless superatoms. The interaction parameters for C–H₂ and H₂–H₂ contacts are the same as used in the previous paper.²² In the interaction models we have included the Feynman–Hibbs quantum correction.^{33,34}

The experimental isotherm has been fitted by simulated ones calculated for infinite slit pores (with infinite graphene walls) of different widths. We assumed that the experimental isotherms are linear combinations of simulated ones, calculated for slit sizes (defined as the distance between positions of the carbon atoms in the slit walls) between 0.7 and 3.0 nm. By this procedure, both total amount stored and the excess isotherms have been well reproduced (Figure 1). The most simple but very accurate fits have been obtained from bimodal distributions of pore sizes with the following widths: 1.3 and 2.0 nm for 3K sample and 0.9 and 3.0 nm for MCS-30 sample, in good agreement with experimental data.³²

ADSORPTION IN CARBON STRUCTURES

Although many models of activated carbon are proposed in the literature, detailed experimental structural characterization of activated carbons is not currently possible. The local structure

in different activated carbons critically depends on the preparation procedure. It is assumed that locally micrographene layers exist, especially in the high-surface-area (above $2000 \text{ m}^2/\text{g}$) activated carbons. Recently it has been concluded that “a best guess at the moment is that the defective micro-graphene layers are dominated by six-member ring systems ... accommodated by ring system of other sizes”.³⁵ However, modeling of such structures is complex, as it must reproduce a large variety of material characteristics such as specific hardness, stable porosity, pore size distribution, energy of adsorption, and many others.³⁵ Therefore, models of slit pores with parallel walls or cylindrical tubes of nanometric diameter have been most frequently used because they give a simple way to interpret theoretical results. We explored slit model characteristics in our previous papers^{4,22} where we have estimated the limits of hydrogen adsorption in slit pore geometry. Here, we compare it with more elaborated geometries that could exist locally: pores of square or triangular section (Figure 2) and

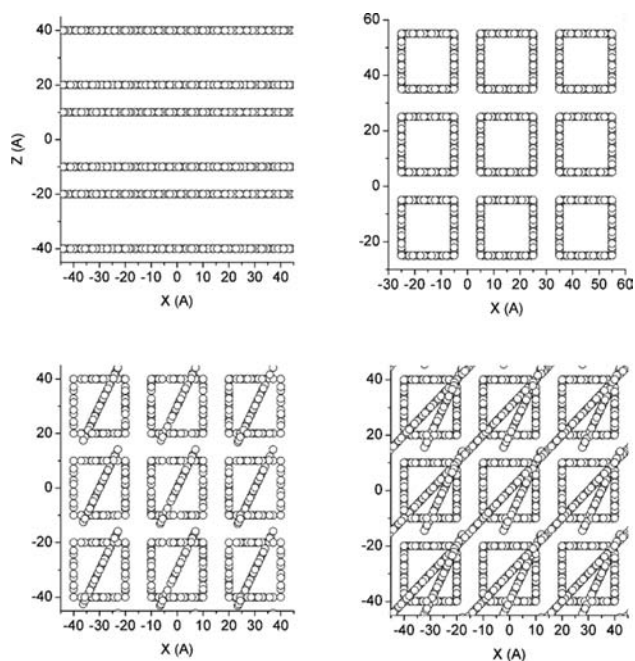


Figure 2. Basic geometries: first row, double slit (DS) and square (SQ); second row, triangular T1 and T2. The figures show projections xz along the y axis.

hypothetical 3D structures with specific surfaces larger than those of graphene. We compare adsorption in these geometries with the reference slit structure composed of two slits of different widths (as the ones found above in the fitting procedure of experimental isotherms). We call it double slit (DS) system. The square and triangular pores have been designed starting from the same DS geometry (see Figure 2).

The conclusion is clear: the pure carbon square and triangular pore shapes do not increase the storage capacity as compared to the slit geometry (Figure 3). A similar conclusion is relevant also for cylindrical structures.^{13,36} In a general way, the structural heterogeneity introduced by different geometries causes a considerable decrease in the total amount of adsorbed gas as compared to ideal slit graphene pores. Although there is no general proof of this statement, there are at least two physical reasons that lead to such behavior. First, some space in heterogeneous pores is usually difficult to access (like pore's

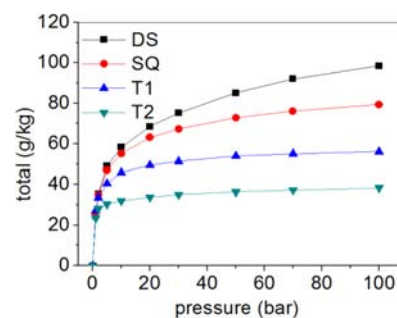


Figure 3. Total adsorption isotherms ($T = 77 \text{ K}$) in geometries from Figure 2.

corners or interstitials in nanotubes), which makes the effective system specific surface area smaller. Second, the decrease of energy of hydrogen adsorption in heterogeneous structures usually leads to smaller uptake.¹² It seems to be a general conclusion: one cannot increase the adsorbed quantity only by topological modification of the slitlike geometry of pores. This conclusion is strongly supported by recent computational study of hydrogen storage in covalently bonded graphenes.³⁷ This 3D structure is not able to adsorb at room temperature more than 4 wt % of hydrogen, even when graphene properties are modified by a dispersion of transition metals inside. We need other options that allow increasing adsorption surface and, if possible, also the adsorption energy.

Historically, the models of structures built of small polycyclic aromatic hydrocarbons have been already proposed.^{13,38–40} It was estimated¹³ that a hypothetical carbon structure built of small molecules can have total surface area 2–3 times larger than the graphene one. We show in our upcoming paper²⁶ that this increase of specific surface of the structure by pore wall fragmentation is accompanied by a substantial decrease of adsorption energy at the pore edges. Both adsorption energy and specific surface area are the most crucial characteristics of materials for hydrogen storage. In the following section we test numerically the limits of adsorption in such systems. The goal will be to propose hypothetical structures that provide guidance for future design and synthesis of highly adsorbing carbons. Such options are explored in the following sections.

■ HIGH-SURFACE-AREA PORE GEOMETRIES

The increasing surface area of small graphene fragments modifies the distribution of the adsorption energy. The additional “edge” surface has lower energy than the infinite graphene layer.²⁶ This competition between increasing surface and decreasing average adsorption energy is the key feature defining the hydrogen uptake in different open geometries, including the MOF-, COF-, or PAF-type structures.

The following three models of porous structures are hypothetical but plausible. They are built with polycyclic aromatic carbons as building units, bonded to form regular 3D structure. We used benzene, coronene, and a hypothetical supramolecule which consists of 43 rings (116 carbons) as shown in Figure 4. The resulting specific surface of the supramolecule (including edges) is about $4600 \text{ m}^2/\text{g}$: it is much more than the surface of graphene layer but also less than the surface of benzene and coronene (both are above $6000 \text{ m}^2/\text{g}$). In fact the specific surface of benzene and coronene are mostly due to the edge surface component whereas the hypothetical supramolecule has only half of its surface coming from the edge contribution.

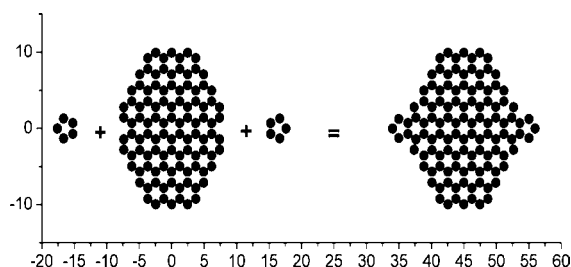


Figure 4. Polycyclic aromatic hydrocarbon supramolecule used to construct hypothetical carbon porous systems. The size of the supramolecule has been chosen to provide comparable edge and in-plane surface. The axis scales are in angstroms.

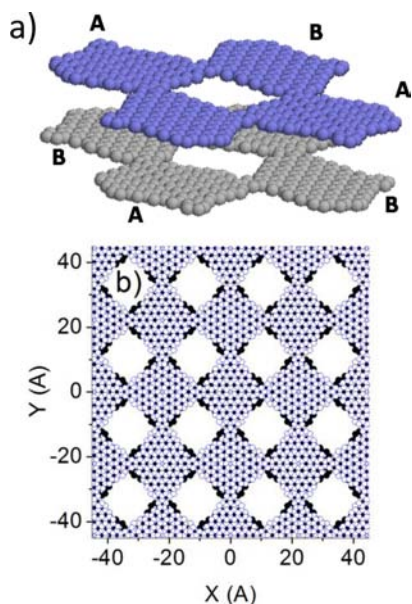


Figure 5. Hypothetical carbon “open” 3D patch porous structures. (a) Basic unit of the pore consisting of eight supramolecules. The long axes of molecules A and B are orientated perpendicularly to each other. (b) 3D structure that possesses infinite slit pore geometry. The molecules in the subsequent walls in the z direction follow ABAB sequence. Two different colors have been used to make better contrast between two walls and have no physical meaning.

Two hypothetical 3D structures (Figures 5 and 6) have been defined by using only the supramolecule from Figure 4. We call the first one 3D patch structure (Figure 5). It has slit-type geometry with the slit walls built of bonded supramolecules (Figure 4). This structure is periodic with the lattice constant $a = 4.432$ nm in x and y directions and slit width d in the z direction. The unit cell contains four supramolecules, in the volume $V_1 = a^2d$. The second model (Figure 6) is a 3D orthorhombic ordered periodic structure with pseudocubic cell ($a = b = c = 4.432$ nm). It contains six supramolecules in the volume of the unit cell ($V_2 = a^3$). In consequence, the 3D orthorhombic system has always lower density than the 3D patch structure, unless $d > 2a/3$.

RESULTS

Figure 7 compares adsorption in the 3D patch and 3D orthorhombic structures. The total adsorption shows impressive storage capacity, especially for the 3D orthorhombic structure. It is instructive to compare this result with the hydrogen uptake reported recently for PAF high-capacity

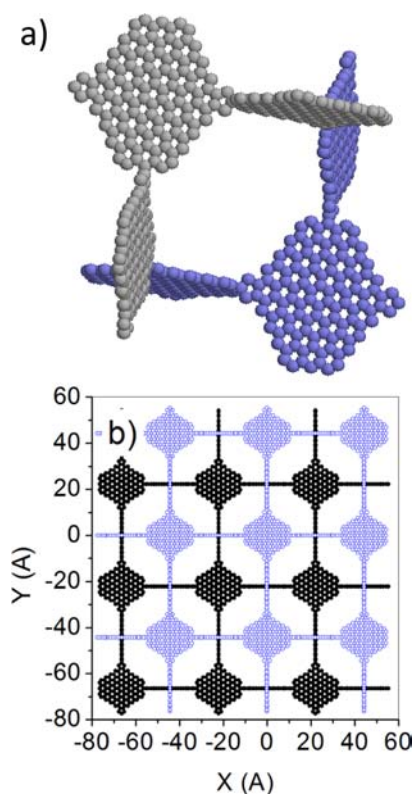


Figure 6. Hypothetical carbon porous 3D orthorhombic structures. (a) Basic unit of the structure consisting of two bonded subunits (gray and blue symbols), which are shifted along the z direction with respect to each other. Each subunit consists of three bonded supramolecules having three different (perpendicular) orientations (in xy , xz , and yz planes). Two subunits are bonded together. (b) 3D orthorhombic structure with a period equal to the distance between the centers of neighboring supramolecules having the same orientation.

systems.³¹ The total gravimetric adsorption in both structures is almost comparable but our hypothetical systems perform better (22.38 wt % for PAF-304 versus 26 wt % for 3D orthorhombic). Even more interesting, a difference is also observed in excess adsorption (8.42 wt % for PAF-304 at 60 bar and 8.6 wt % for 3D orthorhombic at 60 bar). The excess adsorption in the 3D orthorhombic structure is about 10% larger than in the 3D patch topology due to very open orthorhombic structure where all edges are easily accessible for the adsorption. It is important to remember that specific surface of 3D orthorhombic structure is much smaller than that of PAF-304 (because the latter one is built essentially from benzene molecules, which have larger component of the “edge” surface).

The adsorption simulated at 77 K shows that the proposed OCF structures offer a possibility of efficient hydrogen storage. From the point of view of practical applications, room-temperature storage is the most important property. Figure 8 shows the adsorption isotherms for both 3D structures, simulated at room temperature ($T = 300$ K). Depending on a structure, the total uptake is between 15 and 45 g/kg. However, if a hypothetical potential model with doubled strength of hydrogen–pore wall interaction is applied (corresponding to the energy of adsorption of 9 kJ/mol on graphene), the total uptake increases to between 30 and 60 g/kg. The excess adsorption is even more sensitive to variation of adsorption energy (see Figure 8b). This simple comparison

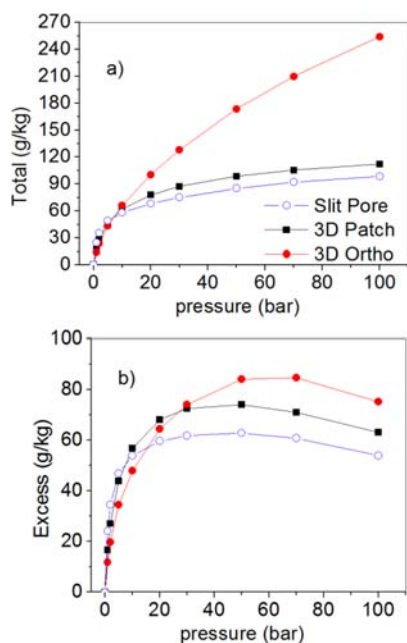


Figure 7. Adsorption isotherms (a, total; b, excess; $T = 77$ K) for two high-surface-area OCF ordered geometries (3D patch and 3D orthorhombic) and for the infinite slit pore. Adsorption in the infinite slit built from graphene walls has been shown for comparison. Pore width $d = 1$ nm for both 3D patch and the infinite slit.

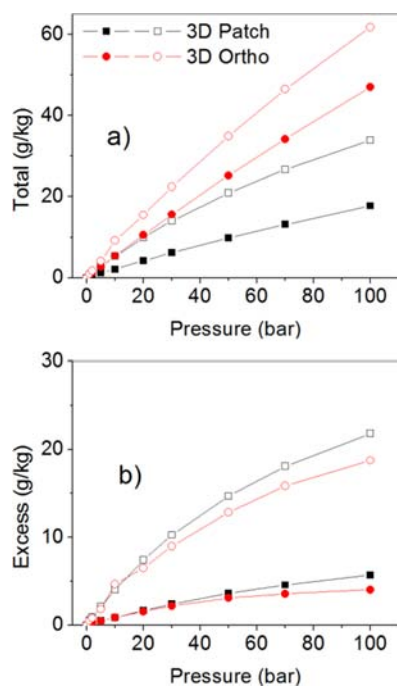


Figure 8. Adsorption isotherms (a, total; b, excess; $T = 300$ K) of two high-surface-area geometries 3D with two models of interaction. (Closed symbols) Basic interaction model (energy of adsorption on graphene equals 4.5 kJ/mol). (Open symbols) Interaction model 2 times stronger than the initial one (that is, 9 kJ/mol). The excess adsorption is very similar in both 3D structures, which is a consequence of similar local (supramolecular) topology.

illustrates the role of surface modification in the process of adsorbent optimization. It also shows that energy of 10–15 kJ/mol will be necessary to reach DOE requirement for mobile applications, even if the adsorbent shows high specific surfaces.

The room-temperature calculations bring an explanation of high storage capacity predicted for the PAF materials (65.3 g/kg in PAF-304 model). The explanation comes from the comparison of interaction parameters applied in our simulation and the ones used for modeling PAF systems. The depth of the interaction curve between H atom (in H_2 molecule) and C atom (in carbon ring) would be 0.0542 kcal/mol in our calculation,²² whereas it was 0.0892 kcal/mol in PAF³¹ systems (and even 0.1120 kcal/mol in COF²⁹ structures studied by the same authors). These parameters are similar as in our double strength potential. In this case, the uptake (Figure 8a) is comparable with the best COF²⁹ and PAF³¹ materials reported in the literature. It means that our hypothetical OCF structures perform better than the COF and PAF geometries because of their topology and despite the smaller accessible surface for adsorption (3900–4400 m^2/g versus 7100 m^2/g in PAF-302).

Figure 9 shows a comparison of distributions of adsorption energies in our OCF structures with a very detailed ab initio

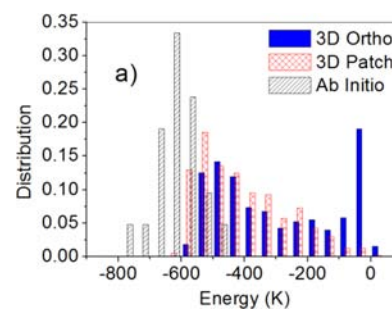


Figure 9. Distribution of the adsorption energy in 3D patch and 3D orthorhombic structures ($T = 77$ K) and from ab initio calculations.⁴¹ (1 kJ/mol = 120.33 K.)

calculation⁴¹ of molecular hydrogen interaction with polycyclic aromatic hydrocarbons, up to coronene. There are a few important features to mention. First, ab initio distribution is shifted toward lower energies. This observation is consistent with the stronger interaction parameters used in literature to calculate adsorption in COF²⁸ and PAF³⁰ systems. The simulated energies (determined from the instantaneous energies in Monte Carlo simulations, $T = 77$ K) have high-energy tails, which represent the molecules being farther from the walls. The high-energy peak for 3D orthorhombic structure represents molecules being practically in the gas phase and interacting very weakly with the carbon walls. Otherwise, all three distributions are similar, which, in addition to experimental verification, proves that our interaction model is coherent with typical ab initio calculations, which usually gives stronger energies of adsorption. The difference between our OCF system and COF or PAF geometries may also result from the local environments (including the influence of heteroatoms). This aspect requires more studies.

There is another logical extension of the analyzed structures to explore. Instead of using relatively large (116 carbon atoms) supramolecules as structure building blocks, we could use PAH molecules, which have even larger edge surface contribution to the total adsorbing surface and much higher specific surface. So, we constructed and tested the third OCF model built from coronene and benzene molecules (Cor_Benz, Figure 10).

This structure has a specific surface of 6500 m^2/g , about 70% larger than the OCFs built from the supramolecule. Does it lead to adsorption uptake that could be much higher? The results of

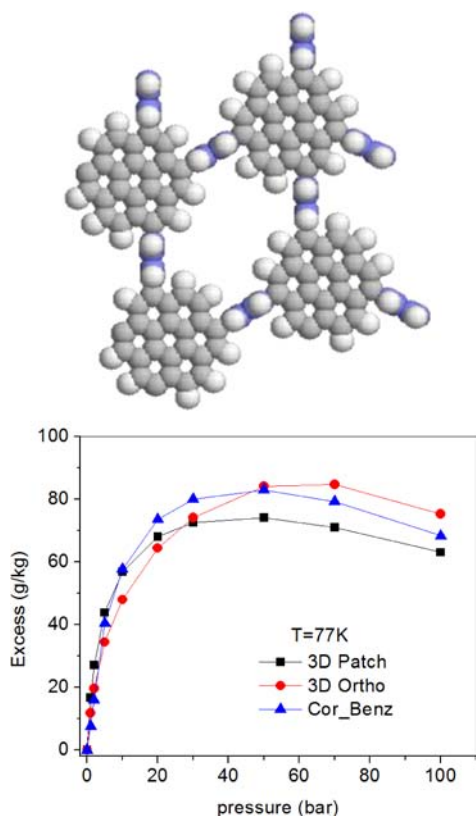


Figure 10. OCF structure built from coronene (shown in gray) and benzene (shown in blue) molecules. Benzene molecules are perpendicular to the plane of coronene molecules. The OCF 3D structure is built from parallel planes defined by the coronene molecules (slit-type structure). The excess uptake of hydrogen in Cor-Benz structure with walls separated by 1.2 nm is larger than in infinite slit pores and 3D patch structures having the same wall separation (about 30% and 13% larger, respectively). At the same time, the maximum value of the Cor-Benz excess adsorption is comparable with that observed in 3D orthorhombic pores. The bulk densities are 0.48, 0.38, and 0.16 g/cm³ for 3D patch, Cor-Benz, and 3D orthorhombic structures, respectively.

adsorption simulations are presented in Figure 10 and the answer is negative. The excess adsorption is in the same range as for the previous OCF structures. In fact, smaller PAH molecules have larger specific surface but the average energy of adsorption is lower, mostly because of the large edge contribution.²⁶ This leads to the result presented in Figure 10, which shows that further increasing the edge contribution does not lead to a substantial increase of hydrogen uptake.²⁶ This is also the main reason why it is difficult to increase the hydrogen uptake in other porous materials like MOFs and COFs. This observation requires additional comments. The main factor limiting increase of adsorption for high-surface-area structures (our OCF Cor_Benz, but also many MOF and COF systems) is the small energy of adsorption in the structures built of small molecules or graphene fragments. For example, the average energy of adsorption at 77 K is about 4 kJ/mol on infinite graphene wall pore but only 3.9 and 3.2 kJ/mol in our OCF systems (3D Patch and Cor_Benz, respectively). So, the smaller energy of adsorption is one of the factors limiting hydrogen storage in high-surface-area carbon-based adsorbents. This implies that the surface may need additional chemical modification to increase the adsorption energy before any applications for mobile hydrogen storage could be considered.

To investigate the stability of the proposed OCF structures, we performed density functional theory (DFT)^{42,43} calculations on the Cor-Benz model, via the ultrasoft pseudopotential and plane-wave approach. The calculations were performed with the Quantum Espresso package.⁴⁴ The exchange–correlation functional used was that proposed by Perdew, Burke, and Ernzerhof,⁴⁵ and the cutoff energy for the plane-wave basis set was included up to 30 Ry. The geometrical parameters of the OCF (which contains 208 atoms), including the cell parameters, were optimized and the cohesion energy was calculated at 0 K. The 3D pore network was found to be stable, with no rotation of the molecules with respect to each other that would lead to a decrease of the surface area and/or pore deformation. The cell remained orthorhombic during the optimization. The cohesion energy at 0 K of the crystal equals 6.3 eV/atom [607.7 kJ/(mol·atom)] which makes the structure stability comparable to most of the common crystals.

Numerical prediction of hydrogen uptake is a delicate procedure. New structures require new force fields, which should be calculated by ab initio methods. The interaction parameters coming directly from these calculations very often require some semiempirical tuning. For this reason, in this paper we have used only the interaction parameters that have been initially tested versus experimental measurements. From such perspective the recent exceptional predictions of enhanced storage capacity of covalent organic frameworks (COF) materials²⁹ and porous aromatic frameworks (PAF)³¹ could be attributed to the fact that the COF and PAF interaction parameters came directly from ab initio calculations, which tend to overestimate the interaction energy by 20–30% (see Figure 9).

The model materials presented in this paper have not been practically synthesized yet. Therefore, the present discussion of possible storage is purely hypothetical. We show one possible way of searching for new porous carbon-based structures with properties required for successful applications.³ The proposed open carbon frameworks have intermediate structures between model slit pores built of graphene infinite walls and COF, MOF, or PAF, based on chains of the smallest aromatic hydrocarbon molecules. They have specific surfaces comparable with MOFs and COFs but higher adsorption energy. Many other carbon-based molecules that could be used to synthesize the OCF structures already exist: coronene, coranulene, ovalene, or even more exotic structures such as nanoribbons,⁴⁶ hexa-peri-hexabenzob[bc,ef,hi,kl,no,qr]coronene,⁴⁷ or recently synthesized porous organic frameworks.⁴⁸ Now we need to find a way to combine them into stable OCF superstructures. This task is not simple. Fortunately, the structures do not have to be ordered. The important characteristic is that they must be built from nanofragments having important edge surface contribution. Therefore, the synthesis could be approached by a modified conventional KOH activation procedure,³² rapid vapor deposition⁴⁹ or template carbonization method.⁵⁰ It is also possible that new nonconventional approaches will be required. For instance, the ablation⁵¹ of the graphene layer using photoinduced mechanism is an emerging way of synthesis of new carbon structures that should be explored.

CONCLUSIONS

The new open carbon frameworks are hypothetical structures alternative to other types of open pore architectures (MOF, COF, PAF). The presented analysis of the hydrogen adsorption in OCF explores the new perspectives and defines the physical

limits of hydrogen storage in nanoporous carbons by physisorption. First, the porous systems must have an open geometry with considerable contribution of edge surface of the building units, which should be fragments of graphene sheet. The size of the fragments cannot be too small because it leads to low energy of adsorption and decreasing uptake.²⁶ At the same time, they cannot be too large because they need to have important contribution of the edge surface. Second, as the OCF geometries increase, the hydrogen uptake (in excess adsorption) increases by 30–50% compared to pure graphene-based pores; additional increase could be achieved by chemical modifications of the pore surface to increase the energy of adsorption above 10 kJ/mol (see Figure 8). This is particularly important for application at room temperature, where increased energy of adsorption could easily compensate higher kinetic energy of adsorbed molecules. Third, the density of the OCF structures cannot be too low because it would lead to poor volumetric capacity. Our 3D Ortho structure has low density (0.16 g/cm³), which gives a very high total uptake (Figures 7a and 8a), but its volumetric capacity automatically is lower (see Supporting Information). Fortunately in general, it is easy to design OCF structures with densities between 0.4 and 0.5 g/cm³. The 3D Patch structure is one example (0.48 g/cm³), but the Cor_Benz structure can be also tailored to have similar density by variation of the interplane distance.

The presented and analyzed examples emphasize that the optimal hydrogen adsorption cannot be achieved without a simultaneous optimization of both adsorbent surface and its adsorption energy. The effect of higher surface area must be amplified by chemical modification of the surface. In fact, the physical limits of hydrogen adsorption require adsorbents with both adsorption energy larger than 10 kJ/mol (in a sustainable way over the whole surface) and the sorbent specific surfaces much higher than 3000 m²/g observed in the best existing carbons.^{5,32} Only such “minimal” conditions may provide the required adsorbed amount at room temperature. As we show, although the OCF structures having specific surface above 6000 m²/g (like Cor_Benz structure) exhibit increased excess adsorption by about 50% with respect to slit pore geometry, they still require additional structural optimization and higher energy of adsorption to achieve the storage capacity required in mobile applications. The same general conclusion is valid for other types of porous systems such as MOF and COF. However, it is important to emphasize that the OCF structures with comparable density but smaller specific surface than PAF adsorbents show higher storage capacity.

■ ASSOCIATED CONTENT

🔍 Supporting Information

One table listing parameters (density, specific surface, energy of adsorption, excess adsorption at 77 K, and total gravimetric capacity at 77 and 300 K) and one figure showing volumetric capacity of OCF adsorbents. This material is available free of charge via the Internet at <http://pubs.acs.org>.

■ AUTHOR INFORMATION

Corresponding Author

bogdan.kuchta@univ-amu.fr

Notes

The authors declare no competing financial interest.

■ ACKNOWLEDGMENTS

This material is based upon work supported by the Department of Energy Grant under Award DE-FG02-07ER46411.

■ REFERENCES

- (1) U.S. Department of Energy's Energy Efficiency and Renewable Energy Website. https://www1.eere.energy.gov/hydrogenandfuelcells/storage/current_technology.html.
- (2) Jena, P. *J. Phys. Chem. Lett.* **2011**, *2* (3), 206–211.
- (3) Froudakis, G. E. *Mater. Today* **2011**, *14* (7–8), 324–328.
- (4) Kuchta, B.; Firlej, L.; Cepel, R.; Pfeifer, P.; Wexler, C. *Colloids Surf., A* **2010**, *357* (1–3), 61–66.
- (5) Burrell, J.; Kraus, M.; Beckner, M.; Cepel, R.; Suppes, G.; Wexler, C.; Pfeifer, P. *Nanotechnology* **2009**, *20* (20), No. 204026.
- (6) Panella, B.; Hirscher, M.; Roth, S. *Carbon* **2005**, *43* (10), 2209–2214.
- (7) Zubizarreta, L.; Gomez, E.; Arenillas, A.; Ania, C.; Parra, J.; Pis, J. *Adsorption* **2008**, *14* (4), 557–566.
- (8) Meregalii, V.; Parrinello, M. *Appl. Phys. A: Mater. Sci. Process.* **2001**, *72* (2), 143–146.
- (9) Bénard, P.; Chahine, R. *Scr. Mater.* **2007**, *56* (10), 803–808.
- (10) Bénard, P.; Chahine, R. *Langmuir* **2001**, *17* (6), 1950–1955.
- (11) Bénard, P.; Chahine, R. *Int. J. Hydrogen Energy* **2001**, *26* (8), 849–855.
- (12) Bhatia, S. K.; Myers, A. L. *Langmuir* **2006**, *22* (4), 1688–1700.
- (13) Chae, H. K.; Siberio-Perez, D. Y.; Kim, J.; Go, Y.; Eddaoudi, M.; Matzger, A. J.; O'Keeffe, M.; Yaghi, O. M. *Nature* **2004**, *427* (6974), 523–527.
- (14) Kuchta, B.; Firlej, L.; Marzec, M.; Boulet, P. *Langmuir* **2008**, *24* (8), 4013–4019.
- (15) Kuchta, B.; Firlej, L.; Marzec, M.; Boulet, P. *Adsorption* **2008**, *14* (2), 201–205.
- (16) Chun-Sheng, L.; Hui, A.; Ling-Ju, G.; Zhi, Z.; Xin, J. *J. Chem. Phys.* **2011**, *134* (2), No. 024522.
- (17) Kuchta, B.; Firlej, L.; Boulet, P.; Marzec, M. *Appl. Surf. Sci.* **2007**, *253* (13), 5596–5600.
- (18) Ferro, Y.; Marinelli, F.; Allouche, A.; Brosset, C. *J. Chem. Phys.* **2003**, *118* (12), 5650–5657.
- (19) Kim, Y.-H.; Zhao, Y.; Williamson, A.; Heben, M. J.; Zhang, S. B. *Phys. Rev. Lett.* **2006**, *96* (1), No. 016102.
- (20) Firlej, L.; Roszak, S.; Kuchta, B.; Pfeifer, P.; Wexler, C. *J. Chem. Phys.* **2009**, *131* (16), No. 164702.
- (21) Jin, Z.; Sun, Z.; Simpson, L. J.; O'Neill, K. J.; Parilla, P. A.; Li, Y.; Stadie, N. P.; Ahn, C. C.; Kittrell, C.; Tour, J. M. *J. Am. Chem. Soc.* **2010**, *132* (43), 15246–15251.
- (22) Kuchta, B.; Firlej, L.; Pfeifer, P.; Wexler, C. *Carbon* **2010**, *48* (1), 223–231.
- (23) Roussel, T.; Bichara, C.; Gubbins, K. E.; Pellenq, R. J. M. *J. Chem. Phys.* **2009**, *130* (17), 6.
- (24) Nijkamp, M. G.; Raaymakers, J. E. M. J.; van Dillen, A. J.; de Jong, K. P. *Appl. Phys. A: Mater. Sci. Process.* **2001**, *72* (5), 619–623.
- (25) Zhao, Y.; Lusk, M. T.; Dillon, A. C.; Heben, M. J.; Zhang, S. B. *Nano Lett.* **2007**, *8* (1), 157–161.
- (26) Firlej, L.; Kuchta, B.; Lazarewicz, A.; Pfeifer, P. *Carbon* **2012**, submitted for publication.
- (27) Rosi, N. L.; Eckert, J.; Eddaoudi, M.; Vodak, D. T.; Kim, J.; O'Keeffe, M.; Yaghi, O. M. *Science* **2003**, *300* (5622), 1127–1129.
- (28) Sculley, J.; Yuan, D.; Zhou, H.-C. *Energy Environ. Sci.* **2011**, *4*, 2721–2735.
- (29) Cao, D.; Lan, J.; Wang, W.; Smit, B. *Angew. Chem., Int. Ed.* **2009**, *48* (26), 4730–4733.
- (30) Furukawa, H.; Yaghi, O. M. *J. Am. Chem. Soc.* **2009**, *131* (25), 8875–8883.
- (31) Lan, J.; Cao, D.; Wang, W.; Ben, T.; Zhu, G. *J. Phys. Chem. Lett.* **2010**, *1* (6), 978–981.
- (32) Romanos, J.; Beckner, M.; Rash, T.; Firlej, L.; Kuchta, B.; Yu, P.; Suppes, G.; Wexler, C.; Pfeifer, P. *Nanotechnology* **2012**, *23* (1), 015401.

- (33) Sese, L. M. *Mol. Phys.* **1994**, *81*, 1297–1312.
- (34) Sese, L. M. *Mol. Phys.* **1995**, *85*, 931–947.
- (35) Marsh, H.; Rodriguez-Reinoso, F. *Activated Carbon*; Elsevier: Amsterdam, 2006.
- (36) Dimitrakakis, G. K.; Tylanakis, E.; Froudakis, G. E. *Nano Lett.* **2008**, *8* (10), 3166–3170.
- (37) Park, N.; Hong, S.; Kim, G.; Jhi, S.-H. *J. Am. Chem. Soc.* **2007**, *129* (29), 8999–9003.
- (38) Gibson, J.; Holohan, M.; Riley, H. L. *J. Chem. Soc.* **1946**, 456.
- (39) Riley, H. L. *Q. Rev. Chem. Soc.* **1947**, *1*, 59–72.
- (40) Kaneko, K.; Ishii, C.; Ruike, M.; Kuwabara, H. *Carbon* **1992**, *30* (7), 1075–1088.
- (41) Donchev, A. G. *J. Chem. Phys.* **2007**, *126* (12), No. 124706.
- (42) Hohenberg, P.; Kohn, W. *Phys. Rev.* **1964**, *136* (3B), B864–B871.
- (43) Kohn, W.; Sham, L. J. *Phys. Rev.* **1965**, *140* (4A), A1133–A1138.
- (44) Giannozzi, P.; Baroni, S.; Bonini, N.; Calandra, M.; Car, R.; Cavazzoni, C.; Ceresoli, D.; Chiarotti, G. L.; Cococcioni, M.; Dabo, I.; Dal Corso, A.; Fabris, S.; Fratesi, G.; de Gironcoli, S.; Gebauer, R.; Gerstmann, U.; Gougoussis, C.; Kokalj, A.; Lazzeri, M.; Martin-Samos, L.; Marzari, N.; Mauri, F.; Mazzarello, R.; Paolini, S.; Pasquarello, A.; Paulatto, L.; Sbraccia, C.; Scandolo, S.; Sclauzero, G.; Seitsonen, A. P.; Smogunov, A.; Umari, P.; Wentzcovitch, R. M. *J. Phys.: Condens. Matter* **2009**, *21*, No. 395502.
- (45) Perdew, J. P.; Burke, K.; Ernzerhof, M. *Phys. Rev. Lett.* **1996**, *77* (18), 3865–3868.
- (46) Yang, X.; Dou, X.; Rouhanipour, A.; Zhi, L.; Rader, H. J.; Mullen, K. *J. Am. Chem. Soc.* **2008**, *130* (13), 4216–4217.
- (47) Herwig, P. T.; Enkelmann, V.; Schmelz, O.; Müllen, K. *Chem.—Eur. J.* **2000**, *6* (10), 1834–1839.
- (48) Yang, W.; Greenaway, A.; Lin, X.; Matsuda, R.; Blake, A. J.; Wilson, C.; Lewis, W.; Hubberstey, P.; Kitagawa, S.; Champness, N. R.; Schroöder, M. *J. Am. Chem. Soc.* **2010**, *132* (41), 14457–14469.
- (49) Kimura, T.; Koizumi, H.; Kinoshita, H.; Ichikawa, T. *Jpn. J. Appl. Phys.* **2007**, *46*, 703–707.
- (50) Ma, Z.; Kyotani, T.; Liu, Z.; Terasaki, O.; Tomita, A. *Chem. Mater.* **2001**, *13* (12), 4413–4415.
- (51) Jeschke, H. O.; Garcia, M. E.; Bennemann, K. H. *Phys. Rev. Lett.* **2001**, *87* (1), No. 015003.